Planetary boundary layer information from GPS radio occultation measurements

C. O. Ao, T. K. Chan, B. A. Iijima, J.-L. Li, A. J. Mannucci, J. Teixeira, B. Tian, and D. E. Waliser

Jet Propulsion Laboratory
California Institute of Technology
Pasadena, CA, USA
chi.o.ao@jpl.nasa.gov

ABSTRACT

With high vertical resolution and ability to penetrate cloud, the GPS radio occultation measurements are potentially very valuable for the global remote sensing of the Earth's planetary boundary layer (PBL). In particular, the PBL height is a crucial parameter that describes much of the diurnal, synoptic, and climatological processes associated with the PBL in a given region, including its cloud characterization and connections between the surface and free troposphere. However, the global climatology of the PBL is poorly established due to a lack of observational data, particularly over the oceans. Adding to the challenge and complexity of this issue, both from a modeling and observation context, is the fact that the PBL top is often so finely delineated that it is difficult to resolve by the limited vertical grid system in most models and observing systems. In this paper, we present preliminary results from our investigations of PBL height determination from GPS measurements. The specific humidity profiles derived from COSMIC data are utilized in this study. An algorithm for deriving the moisture-based PBL height is described and validated by comparison with nearby radiosonde soundings. The algorithm is then used to derive a seasonally averaged map of PBL height in the tropics and mid-latitudes and compare with ECMWF. The results show the great promise of the technique, although a better understanding of sampling errors and more validation works will be needed to make further progress.

1 Introduction

The unique characteristics of GPS radio occultation (RO) [GPSRO or GPS in short] measurements offer great potential in the remote sensing of the Earth's planetary boundary layer (PBL). First, the GPS signals are in the L-band microwave frequencies, which allow them to pass through clouds and precipitation nearly unaffected. The measurements could, *in theory*, yield refractivity profiles down to the surface. Second, by virtue of their active limb viewing geometry, GPS profiles have very high vertical resolution (~ 100 m), making it possible to delineate the fine vertical structure associated with the top of the PBL. Third, with a sufficient number of receivers in orbit, GPS could provide excellent global coverage as well as full diurnal cycle sampling. These facts were recognized early (*Melbourne et al.*, 1994; *Kursinski et al.*, 1997). However, progress on this area has been hampered due to several issues affecting the accuracy of the retrieved profiles in the lowest few kilometers.

The presence of fine-scale vertical structures of the water vapor in the moist lower troposphere introduces three separate problems: (1) atmospheric multipath; (2) receiver tracking error; (3) elevated duct (also known as the superrefraction layer). The first problem, atmospheric multipath, invalidates the traditional excess Doppler approach of extracting ray bending and impact parameter (*Fjeldbo et al.*, 1971). The problem has since been solved through the use of the canonical transform (CT) method (*Gorbunov*, 2002) or the full-spectrum inversion (FSI) method (*Jensen et al.*, 2003). In addition to unraveling the multipath structure in the signal, these methods also make it possible to achieve vertical resolution better than the Fresnel diffraction limit. The second, receiver tracking error, was found to be the dominant cause of the lower tropospheric refractivity bias observed with GPS/MET data (*Rocken et al.*, 1997), and later in the CHAMP and SAC-C data (*Marquardt et al.*, 2003; *Ao*

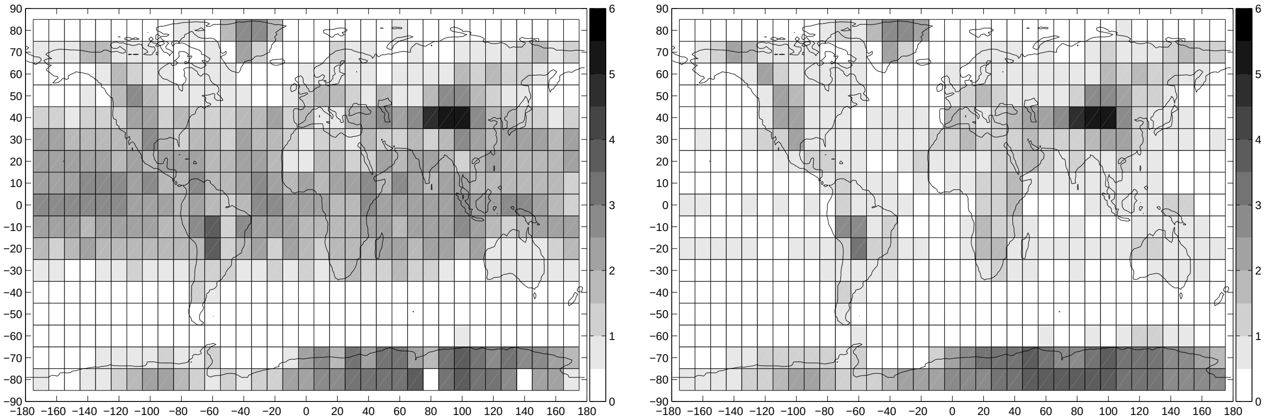

(a) Closed-Loop (b) Open-Loop

Figure 1: Minimum profile heights in km from SAC-C CL data from 2001–2003. The values correspond to the median values of minimum mean-sea-level heights from profiles within each $10^\circ \times 10^\circ$ latitude-longitude box; (b) Minimum profile heights from SAC-C OL data from 2006–2007.

et al., 2003; *Hajj et al.*, 2004). Traditional phase-locked loop (PLL) has proven to be ineffective in dealing with the high amplitude and phase scintillations from the lower troposphere (*Sokolovskiy*, 2001; *Ao et al.*, 2003; *Beyerle et al.*, 2003). This shortcoming has largely been overcome through the use of open-loop (OL) tracking currently deployed on SAC-C and COSMIC (*Sokolovskiy et al.*, 2006b; *Ao et al.*, 2008) as well as the GRAS receiver on Metop-A. The third problem arises from the non-uniqueness of the Abel inversion when ducting or superrefraction condition occurs. In this case, there exists an infinite number of refractivity profiles that give the same bending angle profile, and the Abel-inverted profile is always negatively biased below the duct (*Sokolovskiy*, 2003; *Ao et al.*, 2003; *Ao*, 2007). A practical solution to this problem has not yet been found, although a promising approach has been proposed (*Xie et al.*, 2006).

With recent advances in GPS techniques and instrumentation, several interesting studies that explored the use of GPS data in deriving the top of the PBL have been carried out (*von Engeln et al.*, 2005; *Sokolovskiy et al.*, 2006a, 2007). In this study, we use humidity profiles derived from GPS data to derive the PBL height. In Sec. 2, we discuss the quality of the data. In Sec. 3, we describe the algorithm for extracting the PBL height from GPS data and present some results based on three months of COSMIC data. Our findings are summarized in Sec. 4.

2 Data

With the launch of the six-spacecraft COSMIC/FORMOSAT-3 constellation in April 2006 (*Anthes et al.*, 2008), the volume of GPS data has increased substantially from about 800 to more than 3000 soundings per day. Equally important to the increased number of profiles, COSMIC was designed to acquire GPS data with the OL tracking technology that was developed and tested on SAC-C by JPL (*Sokolovskiy et al.*, 2006b; *Ao et al.*, 2008). OL tracking is crucial for our study because it yields high-quality retrievals much deeper into the lower troposphere and PBL. Fig. 1 shows the comparison between minimum profile heights from closed-loop (CL) vs. OL data from SAC-C. It is evident that OL dramatically improves the sampling in the lowest 4 km altitude, especially over the tropics. Over 80% of the SAC-C OL profiles now reach below 2 km altitude in the tropics, compared to only 50% achieved under CL tracking.

There are various options for defining the PBL heights from GPS data. One can exploit intermediate retrieval products such as the bending angle profile and/or the CT/FSI amplitude (*von Engeln et al.*, 2005; *Sokolovskiy et al.*, 2007). Another option is to use the refractivity (*Sokolovskiy et al.*, 2006a), the fundamental GPS retrieval quantity which is simply related to common meteorological variables. Since GPS measurements are more sensitive to water vapor near the PBL, we have chosen to use the derived specific humidity profile as a basis for PBL height determination. The use of humidity allows for a more direct physical interpretation and more straightforward comparisons with models. The disadvantage is that high-latitude regions where GPS measurements are not sensitive to water vapor would have to be excluded.

Our study makes use of the COSMIC retrievals obtained from JPL's GPS Occultation Analysis System (GOAS) (data available for download from `http://genesis.jpl.nasa.gov`). The mid-to-lower tropospheric humidity profile is derived from the refractivity profile by assuming temperature from the auxiliary source (*Hajj et al.*, 2002). In this case, temperature from the NCEP analysis was used.

Following *Kursinski and Hajj* (2001), the uncertainty in specific humidity q in the lower troposphere can be written in terms of uncertainties in refractivity (N), temperature (T), and surface pressure (P_s) as:

$$\sigma_q = \left[(cT+q)^2 \left(\frac{\sigma_N}{N}\right)^2 + (cT+2q)\left(\frac{\sigma_T}{T}\right)^2 + (cT+q)\left(\frac{\sigma_{Ps}}{P_s}\right)^2 \right]^{1/2} \quad (1)$$

where $c = (a_1 m_w)/(a_2 m_d)$, with $a_1 = 77.6$ K/mb, $a_2 = 3.73 \times 10^5$ K^2/mb, and m_d, m_w are the molecular masses of dry air and water vapor, respectively. The refractivity error term is most significant at the lowest altitudes, while the temperature error term dominates at the higher altitudes.

The dominant contributions to the refractivity error in the lower troposphere are due to horizontal refractivity variations not accounted for by the retrieval method (*Kursinski et al.*, 1997) and the negative refractivity bias arising from the presence of ducts. Both of these effects are more significant over the tropics due to the abundance of water vapor there. In one estimate (*Kursinski et al.*, 1997), the fractional refractivity error increases linearly from 0.2% at 7 km to 1% at the surface. This estimate does not include the effect of ducting, which can be as large as 1% over the tropics (*Ao*, 2007). *Kuo et al.* (2004) analyzed comparisons of CHAMP and SAC-C refractivities with NCEP AVN forecasts and estimated that the GPS surface refractivity error is closer to 3% in the tropics. Thus we consider two scenarios, one in which the surface refractivity error is 1% and one in which it is 3%. The 1% scenario is likely to be more representative of higher latitudes, while the 3% scenario is more representative of the tropics. Assuming 1.5 K temperature error and 3 mb surface pressure error (*Kursinski and Hajj*, 2001), we obtain the meridional distributions of σ_q for the two refractivity error scenarios (Fig. 2), based on the seasonal average q and T atmospheric fields from ECMWF Reanalysis (ERA 40) for the December-January-February (DJF) 2001–2002 period.

To validate the retrieved humidity, we compare the GPS profiles with nearby radiosonde soundings obtained from the Integrated Global Radiosonde Archive (IGRA) (*Durre et al.*, 2006). Considering a maximum separation distance of 200 km and time separation of 2 hr, a total of about 20,000 matches were found between GPS and RAOB for the period from September 2006 to April 2007, about 10% of which are located in the tropics (30 S – 30 N). Fig. 3 shows the RMS fractional refractivity and specific humidity difference between GPS and radiosonde observation (RAOB) computed at the RAOB mandatory pressure levels. Near the surface, the RMS refractivity differences are 2.5% globally and 3.5% over the tropics. The corresponding humidity differences are 1.5 and 2.5 g/kg, respectively. These results appear to be more consistent with the 3% scenario estimate shown in Fig. 2.

3 PBL Height Algorithm and Results

The global PBL varies significantly across different geographical regions, depending on surface properties, surface heat and mass fluxes, and the static stability of the lower troposphere (*Medeiros et al.*, 2005). Given the variety of PBL characteristics, it is a non-trivial matter to define the top of the PBL, especially in deep convective or cloud-topped regions. Models often make use of the bulk Richardson number that detects the temperature inversions at the top of the PBL (*Troen and Mahrt*, 1986). Since GPS measurements are more

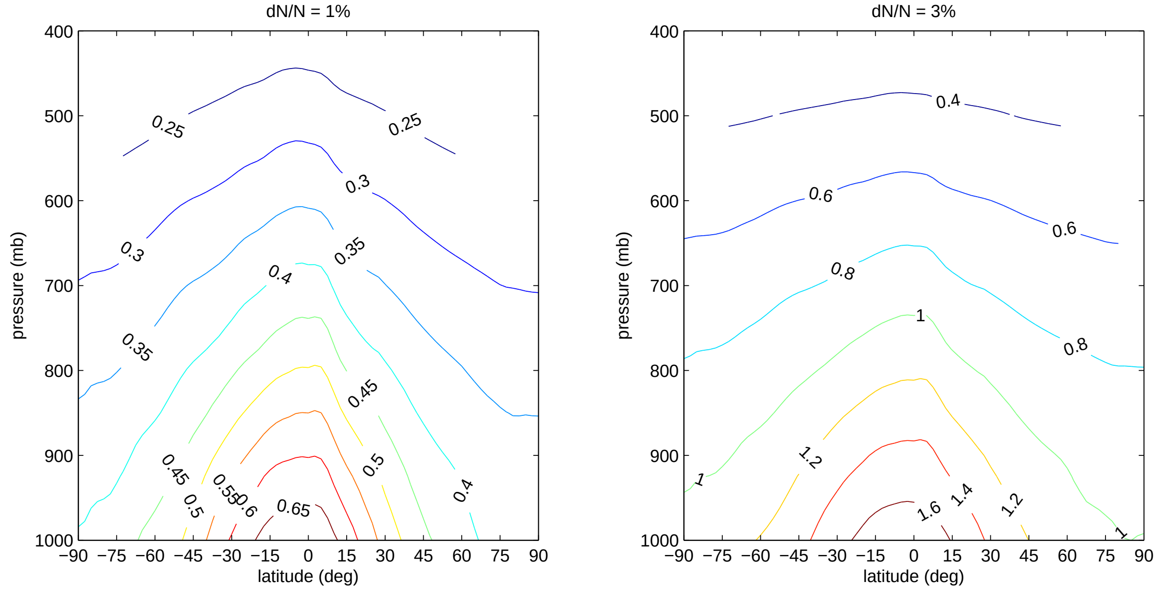

Figure 2: Estimated RMS errors in specific humidity derived from GPS measurements in g/kg for two different scenarios: one in which the surface refractivity error is 1% (left) and one in which it is 3% (right).

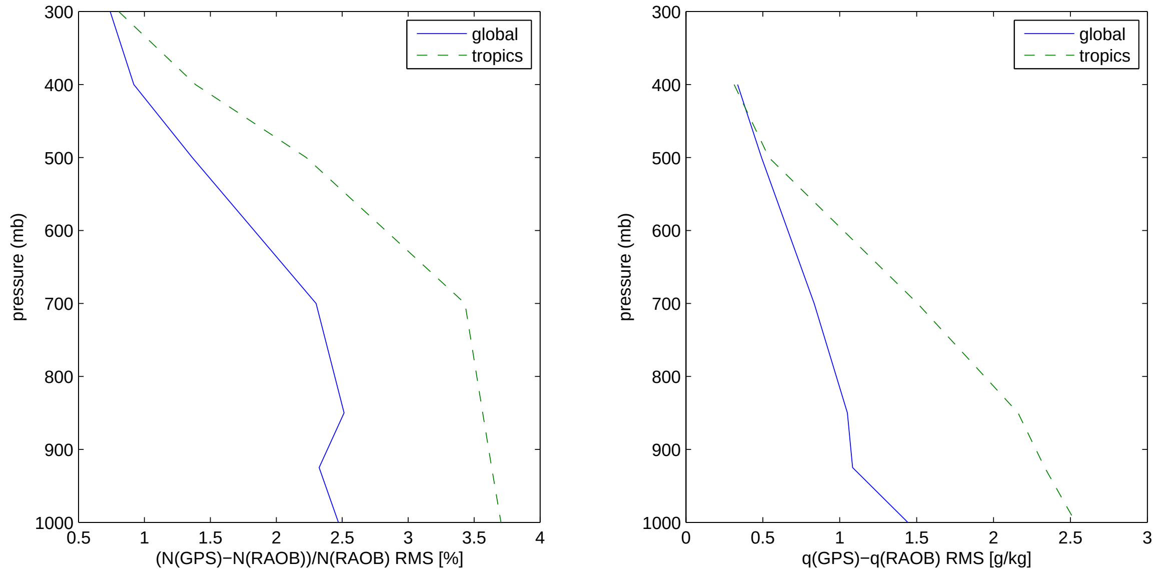

Figure 3: RMS difference between GPS and RAOB fractional refractivity and specific humidity profiles. The GPS and RAOB soundings are located within 200 km and 2 hr of each other. "Global" refers to all latitudes, while "tropics" is restricted to 30 S – 30 N.

sensitive to water vapor near the PBL, an alternative moisture-based definition of PBL height is needed, one that is also amenable to model applications. In this study, the PBL height is estimated to be the height where the minimum of the vertical gradient of the humidity profile dq/dz occurs. This approach is most effective when the PBL is capped with a well-defined inversion layer with the humidity decreasing sharply above the top (e.g., clear convective boundary layer over land or stratocumulus PBL over ocean). However, the local gradient approach could lead to an ambiguous height determination for scenarios where a sharp inversion layer is absent (deep-convective region, residual layer over land, stable PBL) or where the PBL is topped by a cloud layer (e.g., in shallow convective regions over the ocean) or where there are multiple layers in the troposphere with strong gradients.

To validate this approach, we apply the algorithm to specific humidity profiles inferred from GPS and RAOB. For this purpose, we use the U.S. 6-sec radiosonde data that are freely available from the SPARC data center (`http://www.sparc.sunysb.edu/html/hres.html`) (*Wang and Geller*, 2003). The radiosonde profiles in this archive are particularly useful for PBL height comparison because they retain the high vertical resolution of ≈ 30 m, which is much better than the mandatory and significant levels in standard radiosonde archives. For this comparison, we use the separation criteria of 300 km and 3 hr in searching for matchups between GPS and RAOB for the period of Sept. 2006 to Dec. 2006.

Even with OL tracking, GPS profiles do not always reach the surface (cf. Fig. 1). To quantify the effect of incomplete profiles, the PBL heights from RAOB are computed in two ways. In the first case, we limit the RAOB humidity profile to within the the maximum and minimum heights of the GPS profile. The PBL height is then computed from the incomplete RAOB profile. In the second case, the PBL height algorithm is applied directly to the full RAOB profile.

Fig. 4a shows that the PBL heights from GPS and incomplete RAOB agree quite well on average, although considerable scatter exists. The mean GPS-RAOB height difference is 0.36 km, with standard deviation of 1.58 km; the correlation coefficient between GPS and RAOB heights is 0.86. Fig. 4b compares the PBL heights obtained from the incomplete and full RAOB profiles. While they are equal for the most part, the heights from the full profiles are smaller for a fair number of profiles because these profiles capture the stronger humidity gradients missed by the incomplete profiles. For this ensemble, the mean overall PBL height from the interpolated RAOB profiles is higher by about 0.62 km. This suggests that the mean PBL heights inferred from the GPS profiles will tend to be biased high. The actual bias will likely vary from region-to-region depending on the statistics of GPS profile depth penetration and the characteristics of the PBL.

Next, we apply our PBL height algorithm to DJF 2006–2007 COSMIC data and compare with corresponding results obtained from the specific humidity fields of the ECMWF operational analysis. The derived heights are averaged in $10^\circ \times 20^\circ$ latitude-longitude bins. The full ECMWF 6-hour daily fields are used here, i.e., no sub-sampling or interpolation to GPS times, locations, and vertical coverage. To reduce the impact of the aforementioned height bias issue, we include only GPS profiles that reach the lowest 1 km from the surface. Results for the mean and standard deviation are shown in Fig. 5. These results show considerable similarities in morphology between GPS and ECMWF. In general, GPS PBL heights tend to be larger and more variable. However, a careful analysis of sampling bias should be performed before definitive conclusions can be drawn.

Besides the heights of the PBL, it is also interesting to consider how strong the vertical humidity gradients are at the PBL heights. To this end, we define a relative sharpness parameter for each profile as

$$S = (q'_{\min} - q'_{25})/q'_{25} \tag{2}$$

where $q' \equiv dq/dz$, $q'_{\min}$ is the value of q', and q'_{25} is the value of the 25-percentile in q'. The parameter S gives some measure of how distinct the absolute minimum, which defines the PBL height, is compared to the secondary minima in humidity gradients. To see where the "sharp" PBL tops are located, we select profiles in the top 25 percentile in S. Fig. 6 shows the locations of these profiles from the DJF 2006-2007 COSMIC dataset. Also plotted in grayscale is the seasonally averaged vertical velocity (ω) obtained from ERA 40 for DJF 2001–2002 in Pa/s. It can be seen that these "sharp" profiles are predominantly located in the subtropics that correlates strongly with the subsiding branch of the Hadley circulation. This finding is consistent with the

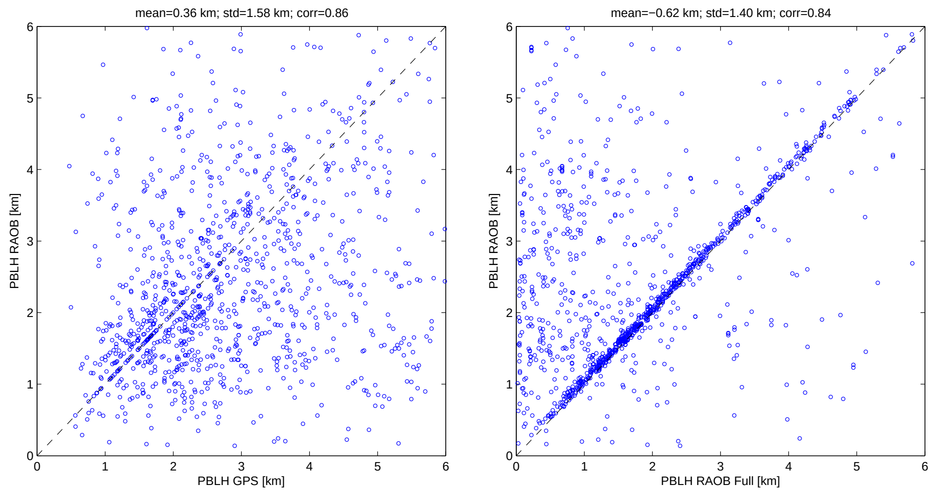

(a) GPS vs. RAOB (b) RAOB full profile vs. RAOB

Figure 4: (a) Comparison between moisture-based PBL heights inferred from GPS and RAOB. RAOB profiles are limited to the GPS heights before applying the PBL height algorithm. (b) Comparison between PBL heights from the incomplete RAOB profiles and the full RAOB profiles.

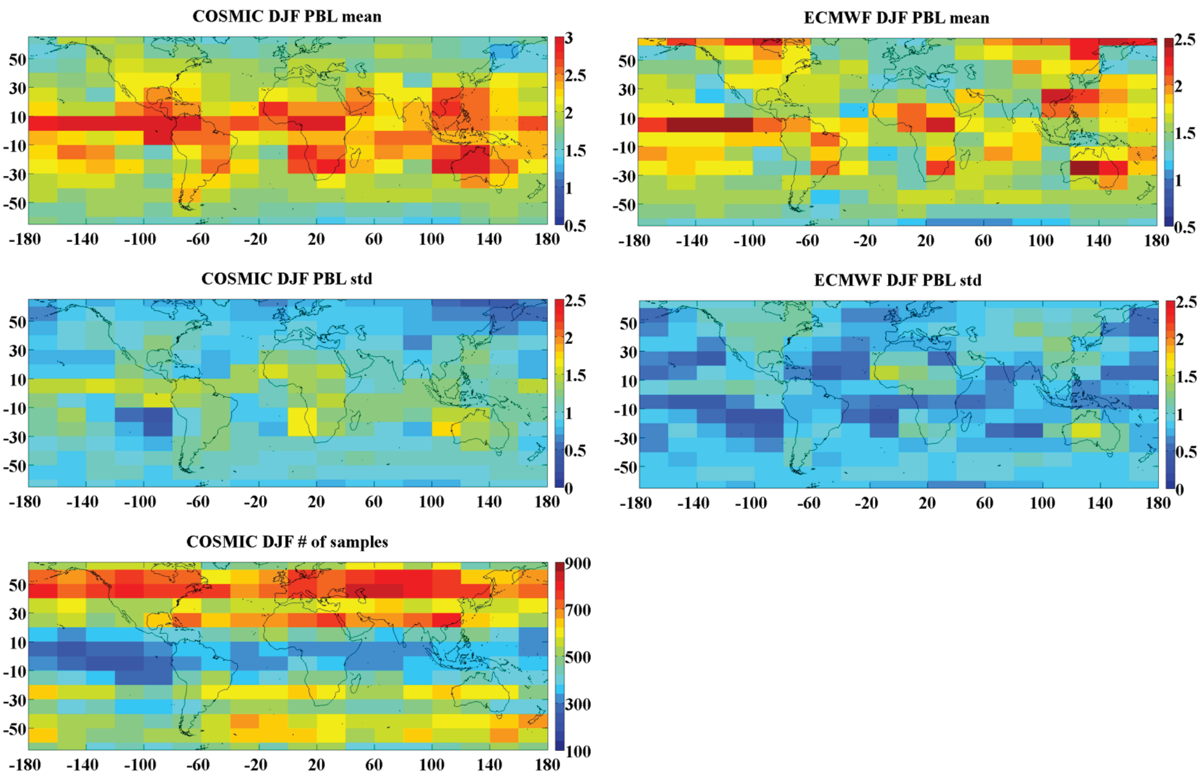

Figure 5: DJF 2006-2007 moisture-based PBL heights in km from GPS/COSMIC and ECMWF. The top panel shows the mean values averaged over $10^\circ \times 20^\circ$ latitude-longitude bins. The middle panel shows the standard deviation. The bottom panel shows the number of GPS profiles averaged in each bin.

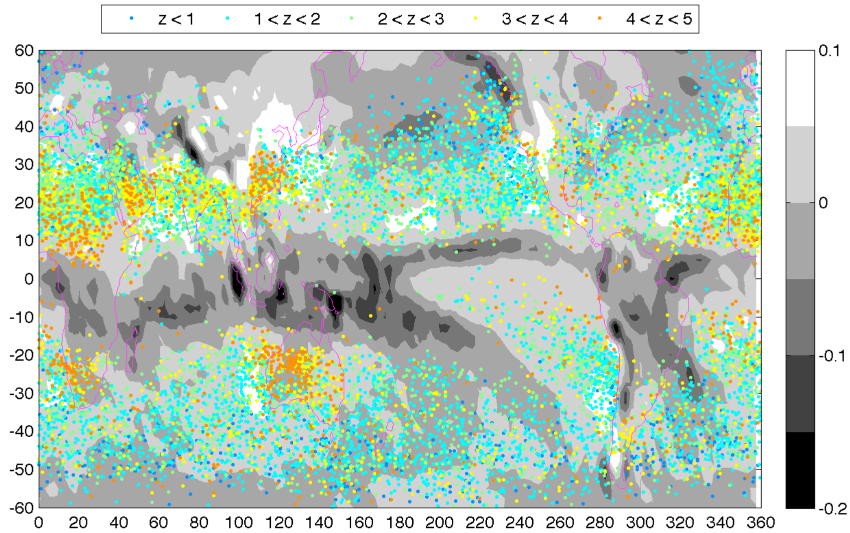

Figure 6: Locations of the top 25 percent profiles in PBL top sharpness. The grayscale map shows the seasonally averaged vertical velocity from ERA 40 for DJF 2001–2002 in Pa/s.

fact that the strongest inversion layers are expected in these regions. The corollary is that the sharp PBL tops are noticeably absent near the Intertropical Convergence Zone (ITCZ) and the South Pacific Convergence Zone (SPCZ). The dearth of "sharp" GPS profiles near the ITCZ has also been reported in *Sokolovskiy et al.* (2007), based on analysis of GPS bending angle profiles.

4 Summary

GPS measurements provide new and exciting opportunities to probe the PBL from space. With recent improvements in retrieval technique and instrumentation, the quality of data in the lower troposphere and the PBL has improved dramatically. The high vertical resolution of GPS profiles can be exploited to delineate the structure of the PBL top. In this study, we considered a moisture-based definition of the PBL height where the PBL height was chosen to be the height for which the vertical gradient of the specific humidity is minimum. This approach is motivated by the fact that the decrease of water vapor from the PBL to the free troposphere is often very large, especially when the PBL is capped with a well-defined inversion layer.

Comparing PBL heights from GPS and nearby radiosonde soundings showed that the heights agree well on average, although considerable scatters were found. Since GPS profiles do not always reach the surface, even with the current improved receiver tracking, the lack of information from the lowest heights could cause some low PBL heights be missed. Thus, PBL heights averaged from GPS profiles could have a positive bias. Comparison of seasonally averaged PBL height from GPS and ECMWF showed strong similarities. However, GPS PBL heights were found to be higher, with larger variance. The higher PBL heights from GPS might be partially due to the sampling bias. Besides PBL heights, we also investigated how large the humidity gradient is at the top of the PBL and the geographical distribution of the sharpest profiles. The GPS profiles with the sharpest PBL tops were found to be strongly clustered in the subtropical subsidence regions, a comforting fact given that strong inversion layers are known to exist in these areas.

These results presented here offer a glimpse of the wealth of unique information that GPS provides on the PBL. They also point to certain limitations of the present technique and the need for future works in algorithm refinement and validation.

Acknowledgements

We thank Drs. Adrian Tompkins and Martin Köhler for providing the ECMWF data. This work was carried out at the Jet Propulsion Laboratory, California Institute of Technology, under a contract with the National Aeronautics and Space Administration.

References

Anthes, R. A., et al. (2008), The COSMIC/FORMOSAT-3 mission: early results, *Bull. Am. Meteorol. Soc.*, *89*, 313–333.

Ao, C. O. (2007), Effect of ducting on radio occultation measurements: an assessment based on high-resolution radiosonde soundings, *Radio Sci.*, *42*, RS2008, doi:10.1029/2006RS003485.

Ao, C. O., T. K. Meehan, G. A. Hajj, A. J. Mannucci, and G. Beyerle (2003), Lower troposphere refractivity bias in GPS occultation retrievals, *J. Geophys. Res.*, *108*(D18), 4577, doi:10.1029/2002JD003216.

Ao, C. O., G. A. Hajj, T. K. Meehan, D. Dong, B. A. Iijima, A. J. Mannucci, and E. R. Kursinski (2008), Rising and setting GPS occultations by use of open loop tracking, *J. Geophys. Res.*, *in review*.

Beyerle, G., M. E. Gorbunov, and C. O. Ao (2003), Simulation studies of GPS radio occultation measurements, *Radio Sci.*, *38*(5), 1084, doi:10.1029/2002RS002800.

Durre, I., R. S. Vose, and D. B. Wuertz (2006), Overview of the integrated global radiosonde archive, *J. Clim.*, *19*, 53–68.

Fjeldbo, G., A. J. Kliore, and V. R. Eshleman (1971), The neutral atmosphere of Venus as studied with the Mariner V radio occultation experiments, *Astron. J.*, *76*, 123–140.

Gorbunov, M. E. (2002), Canonical transform method for processing radio occultation data in the lower troposphere, *Radio Sci.*, *37*(5), doi:10.1029/2000RS002592.

Hajj, G. A., E. R. Kursinski, L. J. Romans, W. I. Bertiger, and S. S. Leroy (2002), A technical description of atmospheric sounding by GPS occultation, *J. Atmospheric and Solar-Terrestrial Phys.*, *64*(4), 451–469.

Hajj, G. A., et al. (2004), CHAMP and SAC-C atmospheric occultation results and intercomparisons, *J. Geophys. Res.*, *109*, D06109, doi:10.1029/2003JD003909.

Jensen, A. S., M. S. Lohmann, H.-H. Benzon, and A. S. Nielsen (2003), Full spectrum inversion of radio occultation signals, *Radio Sci.*, *38*(3), 1040, doi:10.1029/2002RS002763.

Kuo, Y.-H., T.-K. Wee, S. Sokolovskiy, C. Rocken, W. Schreiner, D. Hunt, and R. A. Anthes (2004), Inversion and error estimation of the GPS radio occultation data, *J. Met. Soc. Japan*, *82*(1B), 507–531.

Kursinski, E. R., and G. A. Hajj (2001), A comparison of water vapor derived from GPS occultations and global weather analyses, *J. Geophys. Res.*, *106*(D1), 1113–1138.

Kursinski, E. R., G. A. Hajj, J. T. Schofield, R. P. Linfield, and K. R. Hardy (1997), Observing Earth's atmosphere with radio occultation measurements using the Global Positioning System, *J. Geophys. Res.*, *102*(D19), 23,429–23,465.

Marquardt, C., K. Schöllhammer, G. Beyerle, T. Schmidt, J. Wickert, and C. Reigber (2003), Validation and data quality of CHAMP radio occultation data, in *First CHAMP Mission Results for Gravity, Magnetic and Atmospheric Studies*, edited by C. Reigber, H. Lühr, and P. Schwintzer, pp. 384–396, Springer-Verlag, Berlin.

Medeiros, B., A. Hall, and B. Stevens (2005), What controls the mean depth of the PBL?, *J. Clim.*, *18*, 3157–3172.

Melbourne, W. G., E. S. Davis, C. B. Duncan, G. A. Hajj, K. R. Hardy, E. R. Kursinksi, T. K. Meehan, L. E. Young, and T. P. Yunck (1994), *The Application of Spaceborne GPS to Atmospheric Limb Sounding and Global Change Monitoring*, JPL Publication 94-18.

Rocken, C., et al. (1997), Analysis and validation of GPS/MET data in the neutral atmosphere, *J. Geophys. Res.*, *102*(D25), 29,849–29,866.

Sokolovskiy, S. V. (2001), Tracking tropospheric radio occultation signals from low Earth orbit, *Radio Sci.*, *36*(3), 483–498.

Sokolovskiy, S. V. (2003), Effect of super refraction on inversions of radio occultation signals in the lower troposphere, *Radio Sci.*, *38*(3), 1058, doi:10.1029/2002RS002728.

Sokolovskiy, S. V., Y.-H. Kuo, C. Rocken, W. S. Schreiner, D. Hunt, and R. A. Anthes (2006a), Monitoring the atmospheric boundary layer by GPS radio occultation signals recorded in the open-loop mode, *Geophys. Res. Lett.*, *33*, L12813, doi:10.1029/2006GL025955.

Sokolovskiy, S. V., C. Rocken, D. Hunt, W. Schreiner, J. Johnson, D. Masters, and S. Esterhuizen (2006b), GPS profiling of the lower troposphere from space: Inversion and demodulation of the open-loop radio occultation signals, *Geophys. Res. Lett.*, *33*, L14816, doi:10.1029/2006GL026112.

Sokolovskiy, S. V., C. Rocken, D. H. Lenschow, Y.-H. Kuo, R. A. Anthes, W. S. Schreiner, and D. Hunt (2007), Observing the moist troposphere with radio occultation signals from COSMIC, *Geophys. Res. Lett.*, *34*, L18802, doi:10.1029/2007GL030458.

Troen, B., and L. Mahrt (1986), A simple model of the atmospheric boundary layer; sensitivity to surface evaporation, *Boundary-Layer Meteorology*, *37*, 129–148.

von Engeln, A., J. Teixeira, J. Wickert, and S. A. Buehler (2005), Using CHAMP radio occultation data to determine the top altitude of the Planetary Boundary Layer, *Geophys. Res. Lett.*, *32*, L06815, doi:10.1029/2004GL022168.

Wang, L., and M. A. Geller (2003), Morphology of gravity-wave energy as observed from 4 years (1998–2001) of high vertical resolution U.S. radiosonde data, *J. Geophys. Res.*, *108*(D16), 4489, doi:10.1029/2002JD002786.

Xie, F., S. Syndergaard, E. R. Kursinski, and B. Herman (2006), An approach for retrieving marine boundary layer refractivity from GPS occultation data in the presence of super-refraction, *J. Atmosheric and Oceanic Tech.*, *23*, 1629–1644.